CALCULATION OF RESIDUAL SLOPE DEFORMATIONS AND SATURATION EFFECT IN ASEISMIC ANALYSIS OF EARTH STRUCTURES

by

A.N.Birbrayer[I], L.A.Eisler[II] and A.I.Smiltnec[III]

Described is a method for calculating residual deformation due to earthquakes in dry embankments of cohesionless soils as well as some methods for considering the influence of liquid on the seismic stability of the saturated section of earth structures and foundations. Calculation examples are given.

Seismic stability of earth structures and embankments is to be evaluated with due consideration of the residual deformations and the excess neutral pressure. Methods to solve these problems are briefly stated below. No expanation is given to symbols most commonly used on the problem.

I. Considered is an embankment of height H composed of dry conesionless incompressible soil and resting on a rigid horizontal foundation AF infinitely stretching rightward (Fig. 1). The initial angle of slope α_0 does not exceed the soil internal friction angle φ.

Model tests and instrumental data show that foundation vibrations cause particles to slip along the slope surface which reduces its angle of slope ("flattening" of the slope). Exact calculation of this phenomenon involves mathematical difficulties; approximate solutions available either assume the sliding mass as a rigid body or fail to estimate slope "flattening". An approximate method for the evaluation of "flattening" is presented below.

Let foundation acceleration be defined by the arbitrary law $\ddot{x}=gf(t)$ in which g acceleration due to gravity and $|f(t)|\leqslant\tan\varphi$ (inequality of opposite sense is discussed in /1/). The following assumptions are made for every moment of collapse:

1. The embankment body is separated into three zones (Fig. 1): a) ABC zone where particles move; b) zone to the right of AD in which soil is in the state of subultimate equilibrium ($\tau<\sigma\tan\varphi$); c) infinitesmal zone ACD in which soil is in the state of ultimate equilibrium ($\tau=\sigma\tan\varphi$).

[I] Research Engineer, The B.E.Vedeneev All-Union Research Institute of Hydraulic Engineering (VNIIG), Leningrad, USSR

[II] Head of Research Group, VNIIG, Leningrad, USSR

[III] Head of Research Group, VNIIG, Leningrad, USSR

2. AB, AC, AD are straight lines.

The condition of constancy of the slope cross-sectional area supposes that as the slope collapses the line AB rotates around the fixed point O in the middle of the slope height.

The movement of a mass point system limited in the ABD zone is examined. This system for the two consecutive moments of time is presented in Fig. 2. The system composition is evidently varying: the points in the triangle A_2KA_1 separated from the system and those in the triangle D_1KD_2 jointed to the system.

A set of three equations in three unknowns, viz. α, β (see Fig. 1) and the normal reaction N on the boundary AD can be obtained using the principle of momentum and equilibrium equations for the ACD zone. Excluding N and β from the set a differential equation

$$u''=\left[\sqrt{[u-f(\theta)](u^2+1)-(u')^2(u-\tan\varphi)}-\sqrt{\tan\varphi-f(\theta)}/\cos\varphi\right]^2(u-\tan\varphi)^{-2}-(u+\tan\varphi), \qquad (1)$$

may be obtained in which $u=\mathrm{ctn}\,\alpha$ and differentiation with respect to dimensionless time $\theta=t\sqrt{6g}/\sqrt{H}$ is marked by primes.

Numerical calculation results for three embankments (1 m, 5 m and 20 m high) of the same soil ($\varphi=30^\circ$), with the same initial angle of slope ($\alpha_o=30^\circ$) and the same foundation acceleration $f(t)$ are presented in Fig. 3. The angles of all the three embankments asymptotically tend to the same value of α_{lim}, but the slower this tendency the higher the embankment.

2. The inception of surplus neutral pressures is stipulated by the development of irreversible volumetric deformations in the soil skeleton resulting from dynamic effects . This dependence may be established experimentally by simulating natural conditions of static and dynamic loading of specimens allowing for their possible change in "liquefaction". Data characterizing dynamic loads in effective (σ_{ij}^e), neutral ($-p$) and total (σ_{ij}^t) stress systems as well as data on dynamic movements of solid (u_r) and liquid (u_l) soil components or their combinations simulating simultaneous ($\rho_o u_o=m\rho_r u_r+n\rho_l u_l$ for $\rho_o=m\rho_r+n\rho_l$) and relative ($u=u_l-u_r$) component movement may be received by solving dynamic problems using the equations of motion of saturated soils /2, 3/. Inclusion of the expression for the percolation friction force $F_{rl}=nT$ presented as a volume force integral operator $X(t)=(\rho_l)^{-1}\mathrm{grad}\,P(t)-\ddot{u}_r+g$ into these equations allows to take into account a comparatively wide range of variations in seismic motion frequency and solid particle size (i.e. permeability coefficient k_f).

In Fig. 4 by way of example presented are the results of the solution to a one-dimensional problem on the effective stresses σ^e under the propagation of steady-state longitudinal vibrations.

If the dynamic component $\mathrm{grad}\,P$ can be neglected, inertia forces in a structure $\Pi_e^\sigma=(\partial\sigma_{ij}/\partial x_j)\vec{e}_i$ may be defined as the product of the soil density and the skeleton acceleration ($\ddot{u}_r$). For steady-state vibrations $\Pi_e^\sigma=[m\rho_r+n\rho_l\Omega(B)]\ddot{u}-m(\rho_r-\rho_l)g$ where $\Omega(B)$ is a function decreasing from 1 to 0 and B the similarity criterion of the phenomena discussed.

For soils with $k_f \leqslant 0.1$ cm/sec under seismic action the inequality $(k_f/ng)^2|\ddot{X}(t)| \leqslant |X(t)|$ proves valid for all the practical cases. Thus $T=\rho_B(X-k_f\dot{X}/ng)$ and the equations may be simplified considerably. In terms of velocities $V_0=\dot{u}_0$, $\tilde{V}=\dot{\tilde{u}}$ these equations become

$$\left.\begin{aligned}
&\rho_0\frac{\partial^2 V_0}{\partial t^2}-(\rho_0 a_g^2-\mu)\,\mathrm{graddiv}\,V_0-\mu\Delta V_0=\left(M+\mu\frac{n\rho_t}{\rho_0}\right)\mathrm{graddiv}\,\tilde{V}-\mu\frac{n\rho_t}{\rho_0}\Delta\tilde{V}\\
&\frac{\rho_B k_f}{\rho_0 g}\frac{\partial^2\tilde{V}}{\partial t^2}+\frac{m(\rho_r-\rho_t)}{\beta\rho_B g}a_g^2 k_f\,\mathrm{graddiv}\,\tilde{V}-\frac{\partial\tilde{V}}{\partial t}=\frac{k_f}{ng}\left[\frac{\partial^2 V_0}{\partial t^2}-\frac{\rho_0 a_g^2}{\beta\rho_B}\,\mathrm{graddiv}\,V_0\right]
\end{aligned}\right\}\quad(2)$$

$$M=mn(\rho_r-\rho_t)a_g^2-n(\lambda+2\mu);\quad \beta=1+n\frac{(\lambda+2\mu)(k_r-k_t)}{k_r k_t}+\frac{4}{3}\frac{M}{k_r},$$

where

a_g^2 - propagation velocity of longitudinal waves for $k_f=0$;

λ and μ - constants of Lame for the skeleton;

k_r and k_t - volumetric compression moduli of liquids and solid particles.

If $\tilde{V}\to 0$ and $k_f\to 0$ the equations can be further simplified. On evaluating V_0 and $\tilde{V}$ effective and other stresses can be calculated.

To illustrate the method calculation results of the simultaneous process of generation and dissipation of excessive neutral stresses (u) are presented in Fig.5. The calculation results are compared with the test data also presented as a diagram. The calculation was performed by the finite difference method using the differential equation which together with the boundary conditions is presented in Fig.5. The relations $(\lambda+2\mu)= =k_c(\sigma_e)$ and $\dot{\varepsilon}_p=\dot{\varepsilon}_p(\sigma_x^e,\varepsilon_0,t)$ essential for the claculations were obtained by soil sample tests (Fig.6) in which the stress-strain state was equivalent to that of a test shown in Fig.5. The correction of the value $\sigma_x^e(x,t)= \sigma_x^e(x,0)-u(x,t)$, as well as $k_c(\sigma_x^e)$ and $\dot{\varepsilon}_{p0}(\sigma_x^e,\varepsilon_0)$ was made for every calculation step. ε_0 was assumed to be independent of the degree of soil "liquefaction" and its value is constant for a fixed value of x.

The diagrams show fair agreement of the test and calculation data.

---

1. B i r b r a y e r A.N. Evaluation of Residual Deformations in Embankments under Earthquake. - Izvestija VNIIG, v.98, Leningrad, 1972.

2. E i s l e r L.A. On the Problem of Deriving of a Set of Equations of Motion of a Saturated Non-Cohesive Soil as a Multicomponent Medium. - Izvestija VNIIG, v.86, Leningrad, 1968.

3. E i s l e r L.A. On the Relation of the Viscous Friction Force and the Pattern of the Dynamic Excitation in Saturated Soil. - Trudy Koordinatsionnyh Soveshchanij po Gidrotehnike, Vyp.47, "Energija" Leningrad, 1969.

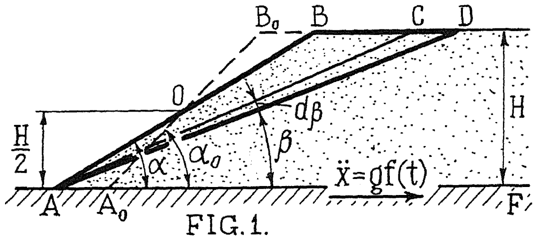

FIG.1.

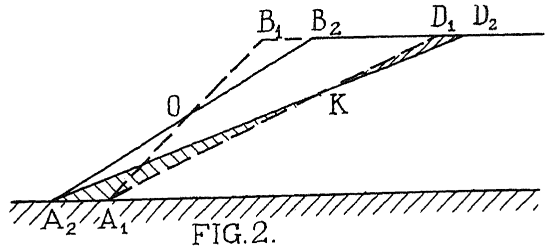

FIG.2.

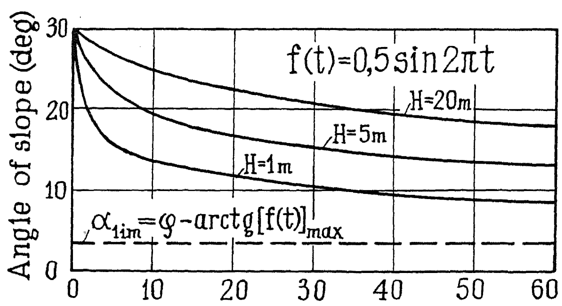

FIG. 3.

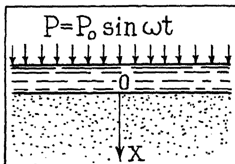

The boundary conditions:

$\sigma_x^e(0,t)=0;\ P(0,t)=P_0 \sin\omega t$

$\sigma_x^e(\infty,t)=P(\infty,t)=0.$

Form of solution:

$$\sigma_x^e(x,t)=A(B)\left\{e^{-\omega\xi_1(B)x}\sin\left[\omega t-\frac{\omega x}{a_1(B)}-\varphi(B)\right]-\right.$$
$$\left.-e^{-\omega\xi_2(B)x}\sin\left[\omega t-\frac{\omega x}{a_2(B)}-\varphi(B)\right]\right\},$$

where $B=\frac{\omega k_f}{ng}$

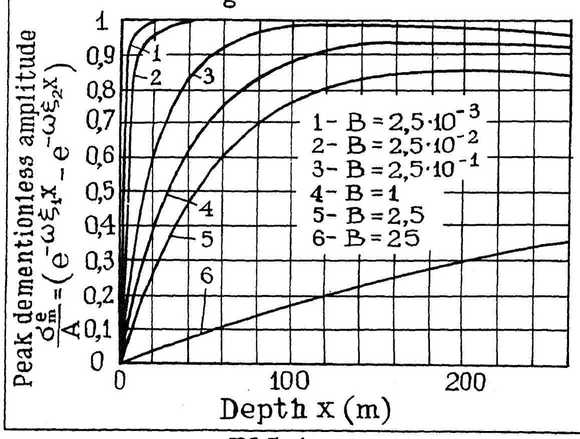

FIG.4.

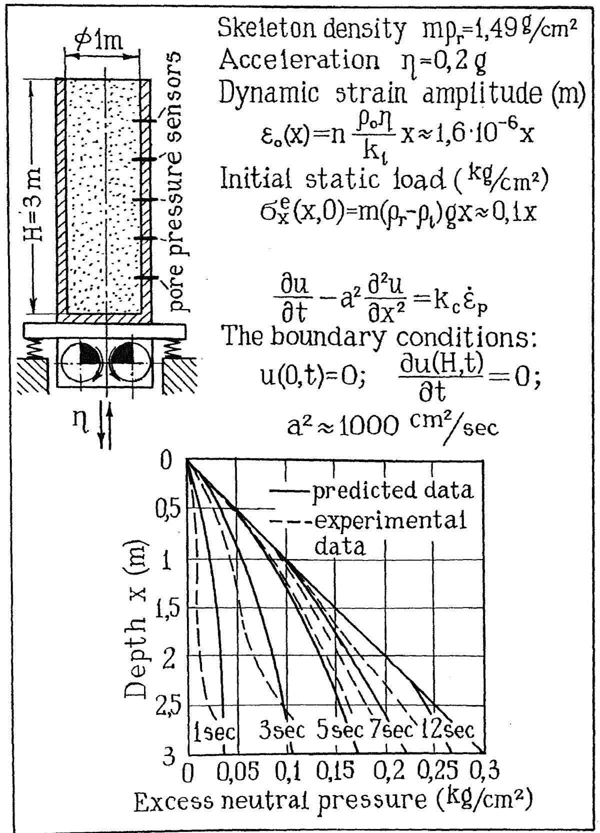

φ1m
H=3 m
pore pressure sensors
η
Skeleton density $m\rho_r$=1,49 g/cm²
Acceleration η=0,2 g
Dynamic strain amplitude (m)
$\varepsilon_o(x)=n\frac{\rho_o\eta}{k_t}x\approx1{,}6\cdot10^{-6}x$
Initial static load (kg/cm²)
$\sigma_x^e(x,0)=m(\rho_r-\rho_t)gx\approx0{,}1x$
$\frac{\partial u}{\partial t}-a^2\frac{\partial^2 u}{\partial x^2}=k_c\dot{\varepsilon}_p$
The boundary conditions:
$u(0,t)=0;\quad \frac{\partial u(H,t)}{\partial t}=0;$
$a^2\approx1000$ cm²/sec
predicted data
experimental data
1sec 3sec 5sec 7sec 12sec
Depth x (m)
Excess neutral pressure (kg/cm²)

FIG.5.

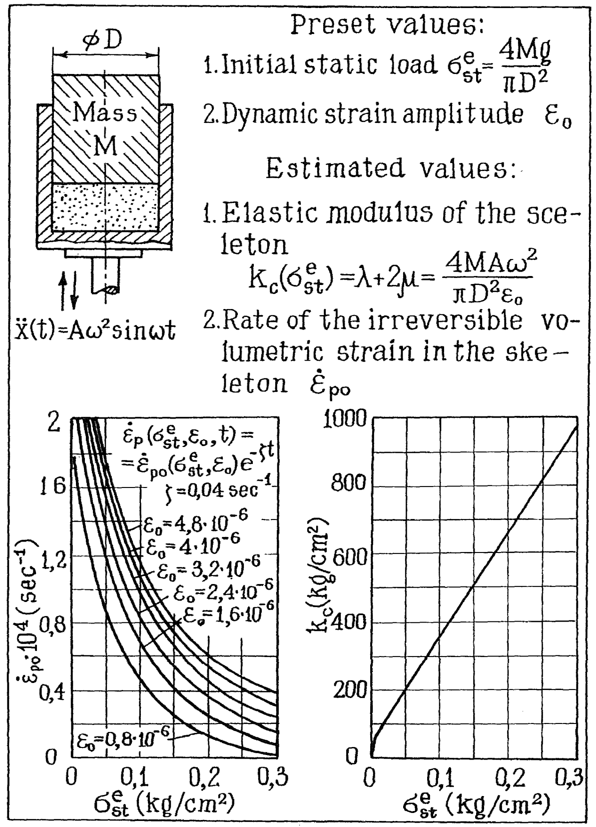

φD
Mass M
$\ddot{x}(t)=A\omega^2\sin\omega t$
Preset values:
1. Initial static load $\sigma_{st}^e=\frac{4Mg}{\pi D^2}$
2. Dynamic strain amplitude ε_0
Estimated values:
1. Elastic modulus of the sceleton
$K_c(\sigma_{st}^e)=\lambda+2\mu=\frac{4MA\omega^2}{\pi D^2\varepsilon_o}$
2. Rate of the irreversible volumetric strain in the skeleton $\dot{\varepsilon}_{po}$
$\dot{\varepsilon}_p(\sigma_{st}^e,\varepsilon_o,t)=\dot{\varepsilon}_{po}(\sigma_{st}^e,\varepsilon_o)e^{-\zeta t}$
ζ=0,04 sec⁻¹
$\varepsilon_o=4{,}8\cdot10^{-6}$
$\varepsilon_o=4\cdot10^{-6}$
$\varepsilon_o=3{,}2\cdot10^{-6}$
$\varepsilon_o=2{,}4\cdot10^{-6}$
$\varepsilon_o=1{,}6\cdot10^{-6}$
$\varepsilon_o=0{,}8\cdot10^{-6}$
$\dot{\varepsilon}_{po}\cdot10^4$ (sec⁻¹)
σ_{st}^e (kg/cm²)
k_c (kg/cm²)

FIG.6.